Robust Control for Independently Rotating Wheelsets on a Railway Vehicle Using Practical Sensors

T. X. Mei and Roger M. Goodall

***Abstract*—This paper presents the development of H_∞ control strategy for the active steering of railway vehicles with independently rotating wheelsets. The primary objective of the active steering is to stabilize the wheelset and to provide a guidance control. Some fundamental problems for active steering are addressed in the study. The developed controller is able to maintain stability and good performance when parameter variations occur, in particular at the wheel-rail interface. The control is also robust against structured uncertainties that are not included in the model such as actuator dynamics. Furthermore the control design is formulated to use only practical sensors of inertial and speed measurements, as some basic measurements required for active steering such as wheel-rail lateral displacement cannot be easily and economically measured in practice.**

***Index Terms*—Active steering, H_∞ control, independently rotating wheelset, railway vehicle, robustness.**

I. Introduction

THE development of electronics has enabled countless applications of advanced control technologies. In the railway industry, one of the significant developments is the use of active controls for railway vehicles. Tilting trains have been successfully used in Europe and the rest of the world, and it appears certain that active secondary suspensions will be widely used. Meanwhile, research work has started in the area of primary active suspensions, where active control is used to steer the railway wheelset for stabilization and/or guidance. A conventional railway wheelset comprises two coned or otherwise profiled wheels joined together by a solid axle. This arrangement has the advantages of natural centring and curving, but when unconstrained it also exhibits a sustained oscillation in the horizontal plane. This is overcome on conventional railway vehicles by means of springs connected from the wheelset to the bogie (truck) or the body of the vehicle. However, this added stiffness degrades the ability of the wheelset to curve and it may cause severe wear of the wheels and rails. Various active methods to steer the solid-axle wheelset have been proposed [1]–[3], where the main aim is to provide necessary stabilization control without interfering with the natural curving action. A major task has been to try and solve the difficult design conflict between the stability, curving performance, and passenger comfort requirements. However, studies have shown that the control demand from actuators can be excessively high [1]. Those design difficulties can be eased and the control demand greatly reduced by allowing the two wheels on the same axle to rotate independently from each other, hence the term independently rotating wheelset (IRW) [1], [4]–[6]. Alternatively, directly steered wheel pairs have been proposed, where two wheels are mounted onto a frame and no axle is required [7]. However, new problems are created with these novel concepts. One of the main drawbacks is that the independently rotating wheelset (or wheel pair) does not have the natural curving ability of the conventional wheelset, and some form of guidance action becomes necessary.

Although several schemes have been proposed for active control of independently rotating wheelsets, some fundamental problems still remain to be solved satisfactorily. One of the first issues for the control design is the measurement difficulty. Active steering for the independently rotating wheelset requires some essential feedback signals such as wheel-rail deflections for guiding the wheelset to follow the track, but a direct measurement of these signals is not feasible in practice. Although state estimation techniques such as Kalman filters can be used to estimate those signals [8], the studies so far have shown that it is extremely difficult to make observers work effectively in the presence of substantial parameter variations.

Another issue that must be addressed is how a control design tackles system uncertainty, which may result from several sources. First, railway vehicles are subject to parameter variations, especially those at the wheel-rail interface such as creep coefficients and wheelset conicity. Second, the dynamics of actuators also add to the uncertainty, as incorporation of the actuator dynamics would tend to make the design process overly complicated. Third, as a railway vehicle is a very complex and nonlinear dynamic system with very high order, a simplified model is normally used for the control design in practice and hence uncertainties due to unmodeled dynamics will have to be guarded against in the design.

In addition, although the design conflict between the stability, curving performance and ride quality is eased by the use of the independently rotating wheelset, it is not completely eliminated. The wheelset instability still exists; the wheelsets must avoid flange contact on curved track; and the passenger ride comfort should be improved.

This paper studies active steering of independently rotating wheelsets using H_∞ design and μ-synthesis and it deals with all the design issues highlighted above. Section II presents a two-axle vehicle that is used in the study and modeling of the vehicle. Formulation and design details of the H_∞ control are

Manuscript received January 26, 2000; revised September 11, 2000. Manuscript received in final form March 9, 2001. Recommended by Associate Editor F. Svaricek. This work was supported by the European Community under Project BE97–4387.

T. X. Mei is with the School of Electronic and Electrical Engineering, University of Leeds, Leeds LS2 9JT, U.K.

R. M. Goodall is with the Department of Electronic and Electrical Engineering, Loughborough University, Loughborough, Leics. LE11 3TU, U.K.

Publisher Item Identifier S 1063-6536(01)04942-9.

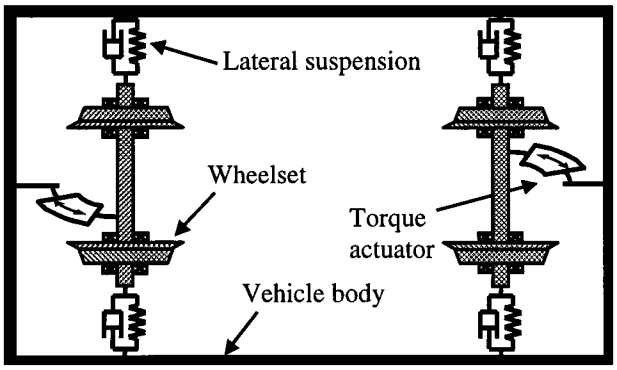

Fig. 1. Plan view of a two-axle vehicle.

given in Section III. Section IV presents and analyzes simulation results.

II. System Description and Modelling

The paper uses a two-axle vehicle for the study, the overall motivation being that the use of active control facilitates a simpler mechanical vehicle scheme than the conventional four-axle vehicle with two bogies (trucks). Because the active steering action only affects the lateral and yaw motions of the vehicle, the plan view model of the vehicle is sufficient for developing active control schemes. Fig. 1 gives a simplified plan view diagram. The modeled scheme mainly consists of a body and two independently rotating wheelsets. The wheelsets are connected to the body via typical springs and dampers in the lateral direction with typical values for a secondary suspension. In practice some form of longitudinal connection is needed to transmit traction and braking forces from the wheels to the vehicle body, but this is not the concern of this study. There are also actuators placed between the wheelsets and the vehicle body in the yaw direction for implementation of active control—these are shown as rotational torque-producing actuators, although in practice they might be a pair of linear actuators.

The plan view model of the vehicle can be represented by (1)–(8), where all variables are related to local track references. All vehicle variables and parameters used in the study are given in Table I. The dynamic complexity of railway vehicle is clearly shown by the equations, particularly in relation to the wheel-rail contact mechanics upon the dynamics of each wheelset. The detail of this is not given here, but can be found in [9]. The equations are all linearized, although in practice substantial nonlinearities may exist if flange contact occurs. The paper uses the linearized models of the wheel-rail contact mechanics exclusively for control law design, principally because nonlinearities are relatively small unless there is flange contact, a condition which active steering avoids—further explanation of this is given in Section IV. The remaining nonlinear effects can be treated as high-frequency structured uncertainty in the H_∞ design approach. Most of simulation results are derived using the designed controllers with a similar linearized model, albeit with parameter variations to represent some of the effects of the nonlinearities. However some simulation results are presented using a nonlinear model in order to validate the appropriateness of the approach which has been adopted.

The model can thus be described by the following equations: Leading wheelset motions (lateral, yaw, and rotation):

$$m_w\ddot{y}_{w1}+\left(\frac{2f_{22}}{V_s}+C_s\right)\dot{y}_{w1}+K_sy_{w1}-2_{f_{22}}\Psi_{w1}-C_s\dot{y}_v - K_sy_v-C_sL_v\dot{\Psi}_v-K_sL_v\Psi_v=m_w\left(\frac{v_s^2}{R_1}-g\theta_{c1}\right) \quad (1)$$

$$I_w\ddot{\Psi}_{w1}+\frac{2f_{22}L_g^2}{V_s}\dot{\Psi}_{w1}+\frac{2f_{11}\lambda L_g}{r_0}y_{w1}+\frac{2r_0f_{11}L_g}{V_s}\dot{\Phi}_{w1} =\frac{2f_{11}L_g^2}{R_1}+\frac{2f_{11}\lambda L_g}{r_0}y_{t1}+T_{w1} \quad (2)$$

$$I_{w1}\ddot{\phi}_{w1}+\frac{r_0^2f_{11}}{V_s}\dot{\phi}_{w1}+f_{11}\lambda\cdot y_{w1}+\frac{r_0f_{11}L_g}{V_s}\dot{\Psi}_{w1} =\frac{r_0f_{11}L_g}{R_1}+f_{11}\lambda\cdot y_{t1} \quad (3)$$

Trailing wheelset motions (lateral, yaw, and rotation):

$$m_w\ddot{y}_{w2}+\left(\frac{2f_{22}}{V_s}+C_s\right)\dot{y}_{w2}+K_sy_{w2}-2_{f_{22}}\Psi_{w2}-C_s\dot{y}_v - K_sy_v+C_sL_v\dot{\Psi}_v+K_sL_v\Psi_v=m_w\left(\frac{v_s^2}{R_2}-g\theta_{c2}\right) \quad (4)$$

$$I_w\ddot{\Psi}_{w2}+\frac{2f_{22}L_g^2}{V_s}\dot{\Psi}_{w2}+\frac{2f_{11}\lambda L_g}{r_0}y_{w2}+\frac{2r_0f_{11}L_g}{V_s}\dot{\phi}_{w2} =\frac{2f_{11}L_g^2}{R_2}+\frac{2f_{11}\lambda L_g}{r_0}y_{t2}+T_{w2} \quad (5)$$

$$I_{w1}\ddot{\phi}_{w2}+\frac{r_0^2f_{11}}{V_s}\dot{\phi}_{w2}+f_{11}\lambda\cdot y_{w2}+\frac{r_0f_{11}L_g}{V_s}\dot{\Psi}_{w2} =\frac{r_0f_{11}L_g}{R_2}+f_{11}\lambda\cdot y_{t2}. \quad (6)$$

Body motions (lateral and yaw):

$$m_v\ddot{y}_v+2C_s\dot{y}_v+2K_sy_v-C_s\dot{y}_{w1}-K_sy_{w1}-C_s\dot{y}_{w2} - K_s\dot{y}_{w2}=\frac{m_vV_s^2}{2}\left(\frac{1}{R_1}+\frac{1}{R_2}\right)-\frac{m_vg}{2}(\theta_{c1}+\theta_{c2}) \quad (7)$$

$$I_v\ddot{\Psi}_v+2L_v^2C_s\dot{\Psi}_v+2L_v^2K_s\psi_v-L_vC_s\dot{y}_{w1}+L_vC_s\dot{y}_{w2} - L_vK_sy_{w1}+L_vK_sy_{w2}=-(T_{w1}+T_{w2}). \quad (8)$$

A state-space form can be readily derived from (1)–(8), as given in (9).

$$\mathbf{x}=A\cdot x+B\cdot u+\Gamma\cdot w \quad (9)$$

where we have the first equation for $\mathbf{x}$ and $\mathbf{u}$ shown at the bottom of the next page.

III. H_∞ Control Design

As described previously, the control design for the active steering is required to meet multiple objectives. It must be able to stabilize the vehicle wheelsets and must do so in the presence of parameter variations and dynamic uncertainty. The wheelsets must be controlled to follow the track with no flange contact allowed on both straight tracks with irregularities and curved tracks—in practice this means restricting the lateral wheel-rail displacement to less than around 8mm. Unlike a solid-axle

TABLE I
VEHICLE VARIABLES AND PARAMETERS

Variables	Definitions and values
C_s	Lateral damping per wheelset (37 kN s/m)
f_{11}, f_{22}	Longitudinal and lateral creep coefficients (nominal 10 MN, range 5-10 MN)
g	Gravity (9.81 m/s^2)
I_v , I_w	Vehicle yaw inertia (558800 kg m^2) and wheelset yaw inertia (700 kg m^2)
I_{wl}	Wheel inertia (100 kg m^2)
K, or K(s)	controller
K_s	Lateral stiffness per wheelset (511 kN/m)
L_g	Half gauge of wheelset (0.7 m)
L_v	Half wheelset spacing of the vehicle (4.5 m)
m_v, m_w	Vehicle mass (30000 kg) and wheelset mass (1250 kg)
P, or P(s)	Vehicle model (the plant)
r_0	Wheel radius (0.45 m)
R_1, R_2	Radius of the curved track at leading and trailing wheelsets (3500 m)
T_{w1}, T_{w2}	Control torque for leading and trailing wheelsets respectively
V_s	Vehicle travel speed (83 m/s)
y_{t1}, y_{t2}	Track lateral irregularity at leading and trailing wheelsets
Y_{w1}, y_{w2}, y_v	Lateral displacement of leading, trailing wheelsets and body
θ_{c1}, θ_{c2}	Cant angle of the curved track at the leading and trailing wheelsets (6^0)
λ	Wheel conicity (nominal value 0.2, range 0.05-0.4)
ϕ_{w1},ϕ_{w2}	Relative rotation angle of two wheels at leading and trailing wheelset.
ψ_{w1},ψ_{w2},ψ_v	Yaw angles of leading, trailing wheelset and vehicle body

wheelset, with IRWs the wheelsets are not required to follow a pure rolling line, but excellent curving performance is still an important requirement because this is difficult to achieve for a passive two-axle vehicle especially when high-speed stability is also required. In addition any control should improve, or at least not worsen, the ride quality of the vehicle.

Fig. 2 shows the structure for the control design and (10) and (11) give the state and output equations that are derived from (9) and formulated for the control design purpose. Note that both input and output vectors are partitioned into two parts.

$$\dot{\mathbf{x}} = \mathbf{A}\cdot\mathbf{x} + \begin{bmatrix}\mathbf{B}_1 & \mathbf{B}_2\end{bmatrix}\cdot\mathbf{u}_{\text{in}} \tag{10}$$

$$\mathbf{y} = \begin{bmatrix}\mathbf{C}_1\\ \mathbf{C}_2\end{bmatrix}\cdot\mathbf{x} + \begin{bmatrix}\mathbf{D}_{11} & \mathbf{D}_{12}\\ \mathbf{D}_{21} & \mathbf{D}_{22}\end{bmatrix}\cdot\mathbf{u}_{\text{in}} \tag{11}$$

where we have the second equation for $\mathbf{y}$ and $\mathbf{u}_{\text{in}}$ shown at the bottom of the page. When designing a controller, it is not necessary to minimize all the states. In fact, designers of a railway vehicle are particularly interested in controlling the lateral wheel-rail displacement and the angle-of-attack (i.e., the yaw angle relative to the track) of the two wheelsets as far as wheelset steering is concerned. Lateral displacement is important because of avoiding contact between the wheel flanges and the rail, and the angle-of-attack affects the lateral creep forces. However, an optimization procedure concludes that it is only necessary to minimize the wheelset lateral displacements [10]. Therefore the lateral displacements of the two wheelsets (y_{w1} and y_{w2}) are defined as the first two variables in the output vector $\mathbf{y}$. The matrix W_{f1} shown in Fig. 2 and given in (12) is a dynamic weighting factor defined to shape the frequency response of the lateral displacement of each wheelset and to maintain stability in the presence of perturbations.

The next two variables in the output vector $\mathbf{y}$ are the two control torques (T_{w1} and T_{w2}), because it is necessary to limit the control effort requirement for practical reasons. The matrix W_{f2} given in (13) is a dynamic weighting factor used as a constraint

$$\mathbf{x} = [\dot{y_{w1}}\ y_{w1}\ \dot{\Psi_{w1}}\ \Psi_{w1}\ \dot{\phi_{w1}}\ \dot{y_{w2}}\ y_{w2}\ \dot{\psi_{w2}}\ \Psi_{w2}\ \dot{\Phi_{w2}}\ \dot{y_v}\ y_v\ \dot{\Psi_v}\ \Psi_v]^{\mathrm{T}}$$

$$\mathbf{u} = [T_{w1}\ T_{w2}]^{\mathrm{T}}\quad \mathbf{w} = \left[\frac{1}{R_1}\ \theta_{c1}\ y_{t1}\ \frac{1}{R_2}\ \theta_{c2}\ y_{t2}\right]^{\mathrm{T}}.$$

$$\mathbf{y} = \begin{bmatrix}y_1\\ y_2\end{bmatrix} = [y_{w1}\ y_{w2}\ T_{w1}\ T_{w2}\ \ddot{y_{w1}}\ \dot{\Psi_{w1}}\ \ddot{y_{w2}}\ \dot{\Psi_{w2}}\ \dot{\phi_{w1}}\ \dot{\phi_{w2}}]^{\mathrm{T}}$$

$$\mathbf{u}_{\text{in}} = \begin{bmatrix}u_1\\ u_2\end{bmatrix} = \left[v_{\text{acc}}\ v_{\text{gyro}}\ v_{\text{acc}}\ v_{\text{gyro}}\ v_{\text{spd}}\ v_{\text{spd}}\ \frac{1}{R_1}\ \theta_{c1}\ \frac{1}{R_2}\ \theta_{c2}\ y_{t1}\ y_{t2}\ T_{w1}\ T_{w2}\right]^{\mathrm{T}}.$$

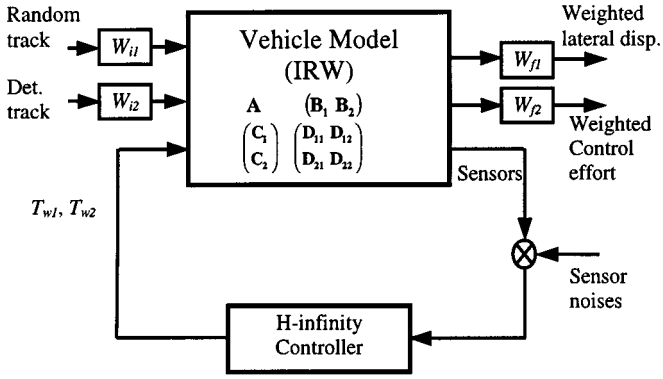

Fig. 2. Structure diagram of H_∞ control design.

on the control torques, in particular to account for the actuator dynamics.

$$W_{f1} = k_1 \begin{bmatrix} \left(\frac{s^2 + 2\xi_{1a}\omega_{1a}s + \omega_{1a}^2}{s^2 + 2\xi_{1b}\omega_{1b}s + \omega_{1b}^2}\right) & 0 \\ 0 & \left(\frac{s^2 + 2\xi_{1a}\omega_{1a}s + \omega_{1a}^2}{s^2 + 2\xi_{1b}\omega_{1b}s + \omega_{1b}^2}\right) \end{bmatrix} \tag{12}$$

$$W_{f2} = k_2 \begin{bmatrix} \left(\frac{s^2 + 2\xi_{2a}\omega_{2a}s + \omega_{2a}^2}{s^2 + 2\xi_{2b}\omega_{2b}s + \omega_{2b}^2}\right) & 0 \\ 0 & \left(\frac{s^2 + 2\xi_{2a}\omega_{2a}s + \omega_{2a}^2}{s^2 + 2\xi_{2b}\omega_{2b}s + \omega_{2b}^2}\right) \end{bmatrix} \tag{13}$$

Selection of output measurements is not straightforward and some natural choices for active steering such as wheel-rail deflection and wheelset angle-of-attack are very difficult and expensive to implement in practice. In this study only practical sensors are used in the design, which are the last six variables defined in the output vector $\mathbf{y}$ measuring the lateral acceleration (accelerometers), yaw velocity (gyros) and relative rotation speed of the two wheels of each wheelset.

There are a total of 14 input variables defined in the input vector $\mathbf{u_{in}}$. The first 12 variables of the input vector $\mathbf{u_{in}}$ all represent disturbances, including sensor noises of the six measurements and track input features. There are two different types of track input. The curve radius (R_1, R_2) and cant angles $(\theta_{c1}, \theta_{c2})$ are the deterministic features, designed to satisfy passenger comfort requirements, whereas the random track inputs (y_{t1}, y_{t2}) are the unintended irregularities, i.e., the deviations from the intended alignment. Special care is needed in the design in order to accommodate these two track features effectively. Input weighting factors (W_{i1}, W_{i2}) are constant weighting matrices defined for the random and deterministic track inputs, respectively, which are used for fine-tuning of the curving performance and ride quality. The last two variables in the input vector are the control input signals $u_2 = [T_{w1}\ T_{w2}]^{\mathrm{T}}$.

If the transfer function from the input disturbances to the output signals (weighted wheelset displacement and control torques) is defined to be $F_1(P, K)$, the design task is then to find a controller K that stabilizes the closed-loop system and minimizes the H_∞ norm of $F_1(P, K)$. This design problem can be readily solved with one of the commercial software packages (in this study the MATLAB toolbox "μ-tools"). The resulting controller is then examined using the μ-synthesis technique to also ensure its robustness against not only the parametric uncertainties, in particular the variation of two parameters which have significant effect on the wheel-rail contact mechanics [9]: the creep coefficient and the wheelset conicity. These two parameters may vary significantly in practice and typically the lateral and longitudinal creep coefficients can be considered to vary between 5MN and 10MN and the wheelset conicity between 0.05 and 0.4 (these are the typical ranges of values which are considered by passive suspension designers). As the parametric sources of the uncertainty are known in this case, it can be readily represented as a structured uncertainty in the form of an inverse additive perturbation with an extra set of input and output connected to a normalized perturbation Δ which is a diagonal matrix with its H_∞ norm less than one [11]. Calculation of the singular value for all channels concerned shows that the maximum single value is less than one and hence the controller satisfies the robustness condition.

By tuning the parameters of all weighting functions, the vehicle performances with the active control can be optimized. Table II gives the final values of all the weighting parameters. The dynamic weighting W_{f1} has been selected to allow the wheelsets to follow the low-frequency (below 10 Hz) elements of the track, which is a compromise between the maximum wheel-rail deflection allowed, and the rejection of high-frequency components of the track and the high-frequency perturbations. The second dynamic weighting W_{f2} has been set to give a cutoff frequency around 12 Hz mainly to reflect the fact that the bandwidth of the current actuator technology feasible for this type of application (hydraulic or electro-mechanical actuators) is normally 15–20 Hz. The coefficients of the two dynamic weightings (k_1 and k_2) are tuned for the overall tracking performance and control effort, where $k_1 = 1$ and $k_2 = 0.8 \times 10^{-7}$ are set in the simulation to meet both requirements. W_{i1} and W_{i2} are constant weighting matrices adjusted to balance the wheelset responses to the random and deterministic track inputs for the passenger comfort and curving performance. W_{i1} is set to unity and the coefficient of W_{i2} is tuned in the simulation to be 0.5—a value which gives the best compromise between the performance on curves and response on random track.

IV. Simulation and Analysis

Fig. 3 shows the diagram of the simulation model used in the study. The weighting factor matrices that were used in the design process are no longer needed and actuator models are now included in order to study the effect of the dynamic effects introduced by the actuators. Simulation results from a passive vehicle with solid-axle wheelsets, which are stabilized by mechanical yaw stiffnesses, are also included for a comparison.

The development of the robust control strategy has been carried out using a linearized model of the railway vehicle, which is justified on the basis that an active steering scheme will improve performance on curves in a manner which considerably reduces the effects of nonlinearities. The nonlinearities of a railway vehicle model are largely associated with nonlinear wheel-rail profiles and contact forces, which become particularly problematic when the wheel-rail contact point approaches the wheel flanges.

TABLE II
PARAMETERS OF WEIGHTING MATRICES

Variables	Definitions and values
k_1	Coefficient of weighting matrices on wheelset lateral displacements (1)
k_2	Coefficient of weighting matrices on control torques ($0.8*10^{-7}$)
W_{i1}	Input weighting matrix on random track input ($W_{i1}= 0.5*\mathbf{I}_{2x2}$)
W_{i2}	Input weighting matrix on deterministic track input ($W_{i2}= 0.5*\mathbf{I}_{4x4}$)
ω_{1a}, ω_{1b}	Frequencies of the dynamic weighting on lateral displacements (15,150Hz)
ξ_{1a}, ξ_{1b}	Damping ratios of the dynamic weighting on lateral displacements (1)
ω_{2a}, ω_{2b}	Frequencies of the dynamic weighting on control torques (20,200Hz)
ξ_{2a}, ξ_{2b}	Damping ratios of the dynamic weighting on control torques (1)

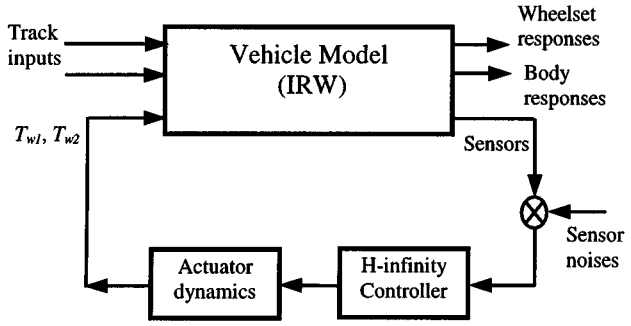

Fig. 3. Simulation model.

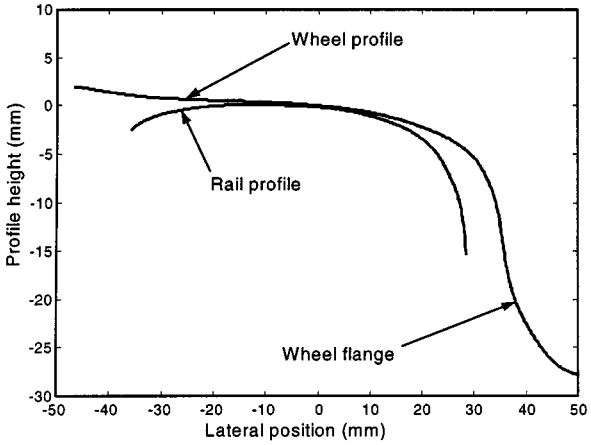

Fig. 4. Nonlinear wheel/rail profiles.

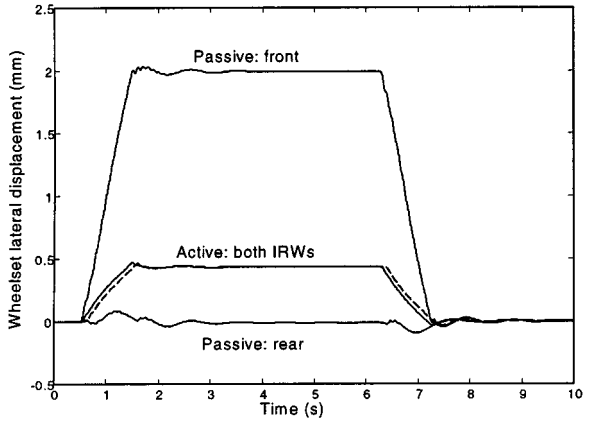

Fig. 5. Wheelset lateral displacement on a curved track ($V_s = 83.3$ m/s).

However, the use of active steering control largely overcomes this problem by steering the wheelset to operate at the linear region of the wheel tread and rail surface. As it will be shown later in the section, the difference between the linearized model and a full nonlinear model is very small for actively steered vehicles. On the other hand, a nonlinear model is essential for simulating passive vehicles on tight curves where flange contact is likely to occur. Although this justifies the use of the linearized vehicle model to assess the vehicle performance of the proposed active scheme, a full nonlinear model is also used in the simulation wherever the difference between the two models becomes significant. The nonlinear model is developed based on the well-known contact theory of Hertz and nonlinear creep theory of Kalker [12]. Also nonlinear wheel/rail profiles shown in Fig. 4 (instead of the coned wheels) are used in the model, which is a standard pair of profiles used by the railway industry.

In the simulation, both deterministic and random track inputs are used to study the responses of the actively controlled vehicles on different tracks. The deterministic track input used for high-speed trains (up to 300 km/h) is defined as a curved track of radius 3500 m with a cant angle of 6°, and having transition sections at both ends with a 1-s duration. A second deterministic track input is used for low-speed curves (vehicle speed 25 m/s), where the curvature radius is 300 m. The random track input represents the roughness of a typical high-speed main line. The generically generated random track input is of a broad frequency spectrum with a relatively high level of irregularities and it will enable a more comprehensive assessment of the proposed active control scheme. On the other hand, measured data from a real track is normally less representative because a specific track tends to have some particular features in a narrower frequency range. Nevertheless, real track data measured from a railway line between Goettingen and Hanover in Germany are also used in the simulation in addition to the generic track input.

On the deterministic track, the active control scheme gives much improved curving performance when compared with the passive vehicle and Fig. 5 shows a typical result. With active control both wheelsets move outwards in the lateral direction close to what would be a pure rolling action for a solid-axle wheelset. However, the wheelsets of the passive vehicle are forced away from the ideal positions by the stabilising yaw stiffness in the opposite directions, an effect which is well known to conventional suspension-designers and which results in increased creepage between the wheels and the track, and hence undesirable wear. Achieving a pure rolling action for

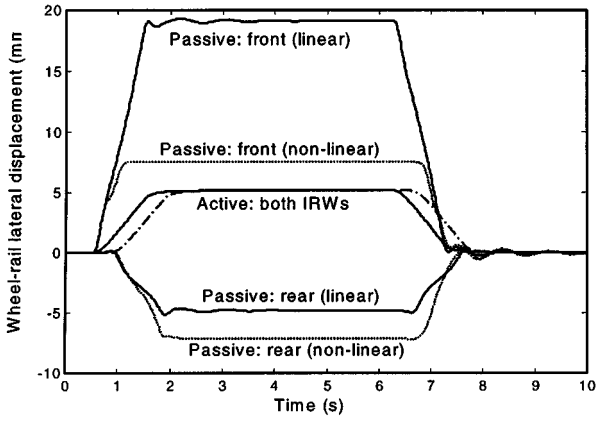

Fig. 6. Wheelset lateral displacement on a curved track ($V_s = 25$ m/s).

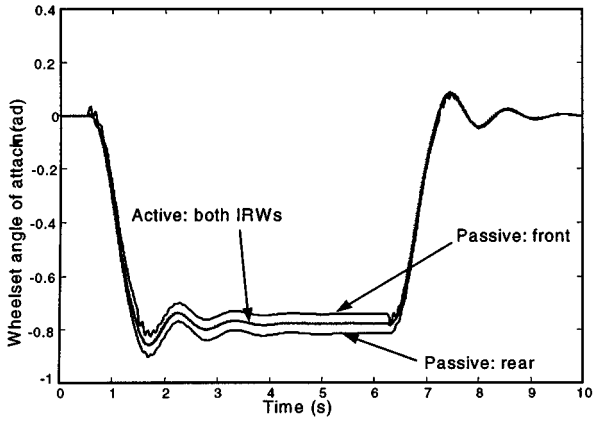

Fig. 7. Wheelset angle of attack on a curved track ($V_s = 83.3$ m/s).

the independently rotating wheelset is not as crucial as for the solid-axle wheelset, as the two wheels on the same axle are allowed to rotate freely and the longitudinal creep force will be much lower. However a good guidance action is required such that the wheelsets follow the track and flange contact is avoided. At lower speed when railway vehicles negotiate tighter curves, the advantage of the active control is even more obvious as indicated in Fig. 6 where the vehicle speed is 25 m/s and the curve radius is 300 m. In this case the large wheel-rail displacement for the passive vehicle from the linearized model would in practice cause flange contact, which is best illustrated using the full nonlinear model as shown in the dotted lines. The hard flange contact for the two wheelsets of the passive vehicle would result in increased creep force and cause damage to both the wheels and the track.

Figs. 7 and 8 show the angles of attack for the two wheelsets for the two curves, and further illustrate the good curving performance achieved by the active control. In both curves the actively controlled wheelsets have the same angle of attack on the steady curve, i.e., just what is required to give the lateral creep which is appropriate for the cant deficiency. By contrast, for the passive vehicle on the low speed curve (Fig. 8), the larger axle rotations mean that irregular angles of attack occur on the curve transitions, whereas they are much more orderly with active control.

On the straight track with random input, the active control also demonstrates excellent tracking performance despite the fact that the wheel-rail deflections are not provided by the

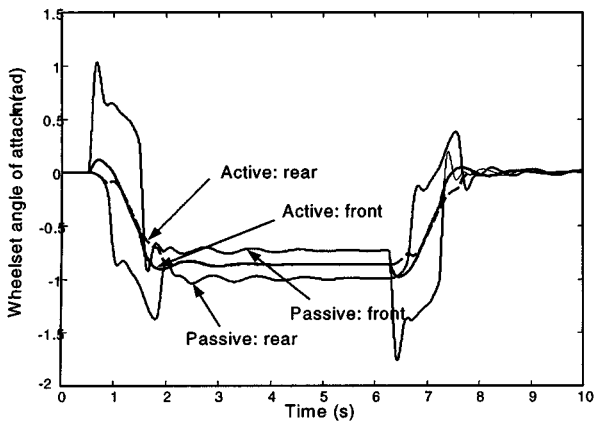

Fig. 8. Wheelset angle of attack on a curved track ($V_s = 25$ m/s).

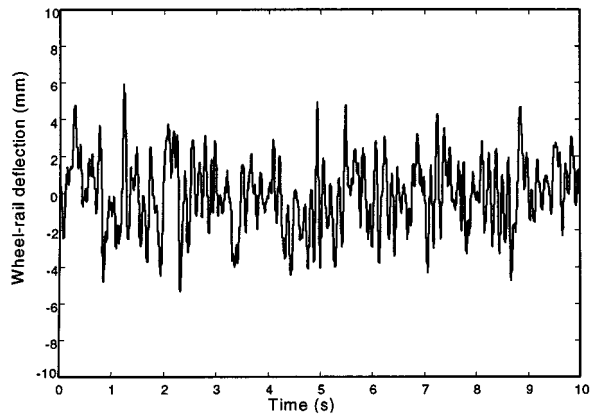

Fig. 9. Wheel-rail deflection on a straight track with irregularities ($V_s = 83.3$ m/s).

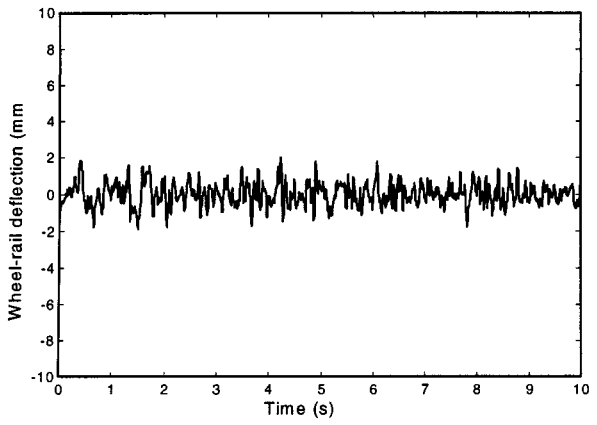

Fig. 10. Wheel-rail deflection on a measured track (Goettingen-Hanover) at $V_s = 83.3$ m/s.

measurement. Fig. 9 shows the lateral displacement of the front wheelset relative to the track at the vehicle speed of 83.3 m/s, where the generic generated track irregularities are used. The maximum deflection is less than 6 mm, which is well within the normal requirement of 8 mm. Because the track irregularity level is proportional to the square of the vehicle speed, the tracking error will be much smaller for lower vehicle speed. For the measured real track data, the condition is much less severe and a maximum wheel-rail deflection of less than 2 mm is obtained as shown in Fig. 10.

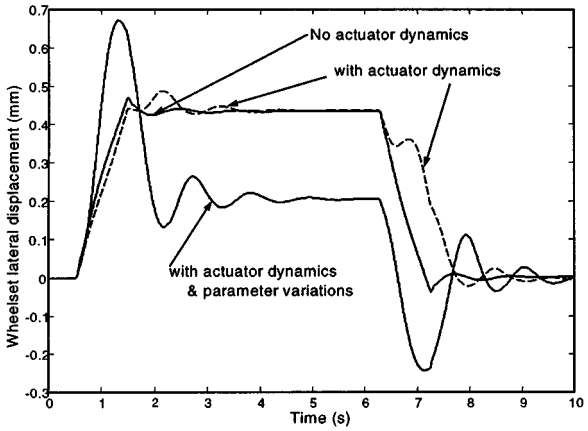

Fig. 11. Robustness analysis ($V_s = 83.3$ m/s).

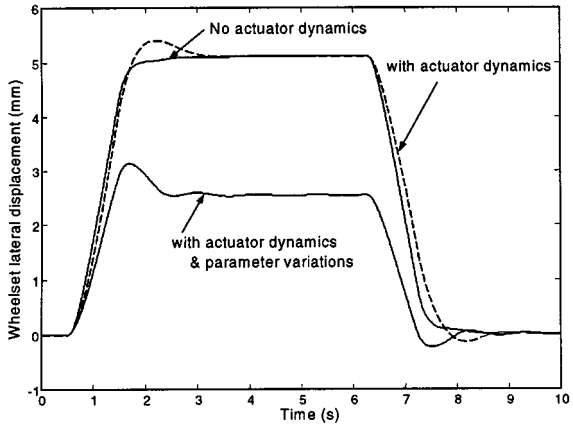

Fig. 12. Robustness analysis ($V_s = 25$ m/s).

One of the critical design aims is that the controller must be robust against the structured uncertainties such as unmodeled actuator dynamics, parameter variations at the wheel-rail interface and nonlinearities of the vehicle dynamics. In this study, a nonlinear model of a hydraulic actuator is used in the computer simulation to assess the performance of the controller. For the parameter variations, a known worst case (the conicity changes from 0.2 to 0.4 and the creep coefficient from 10MN to 5MN) is used. The full nonlinear model is also used to assess the control robustness. Fig. 11 compares the lateral displacements of the leading wheelset on a curved track at the vehicle speed of 83.3 m/s. When the actuator dynamics are considered in the simulation, the wheelset response is delayed and less damped. When the worst parameter variations are also included, the wheelset response shows a relatively large peak on the curve transitions and settles down to its quasistatic level (half of the nominal value because of the larger conicity) on the constant curve. The delay and reduced damping is much less severe for lower vehicle speed. Fig. 12 shows the lateral displacements of the leading wheelset on a curved track at the vehicle speed of 25 m/s. Clearly, the delay caused by the actuator dynamics is much smaller and the peaks on the curve transitions are much lower. In addition, the robust controller is able to reduce significantly the effect of the nonlinearity of the vehicle dynamics. Fig. 13 compares the lateral displacements of the leading wheelset between the full nonlinear (solid line) and the linearized (dashed line) models at the high speed of 83.3 m/s, where the stability is more

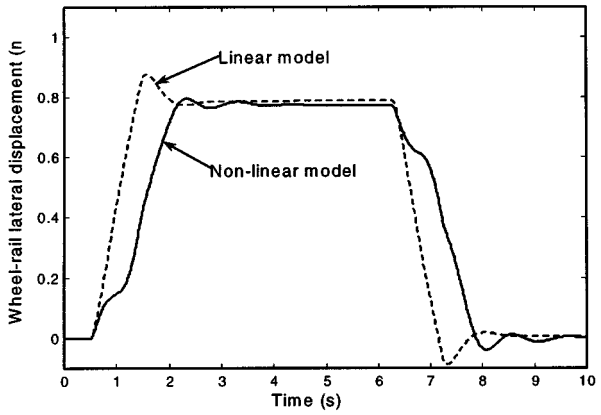

Fig. 13. Wheelset lateral displacement on curves using nonlinear model ($V_s = 83.3$ m/s).

difficult to achieve than at lower speeds. The wheel conicity of the linearized model is reduced from the nominal value 0.2 to 0.11 in order to be close to that of the profiled wheel at the contact region. It is clear from the diagram that the nonlinearity of the wheel-rail contact mechanics is no longer a major factor for the stability of the actively steered vehicle as the active control tends to keep the wheelset operating in its linear section. The wheelset movements from the two models are fairly similar on the constant curve, although the response of the nonlinear model is slightly slower on curve transitions.

Obviously there are some performance differences between the different test conditions, but most significantly the entire closed-loop system is stable in all those circumstances. Several other control structures have been studied for this application under similar design conditions as the H_∞ control, none of which matches the H_∞ control approach developed as far as the robustness issue is concerned. One of those controllers developed is the linear-quadratic optimal approach. While it achieves good performances on both curved and random tracks with ideal actuators, the LQ optimal controller becomes unstable (results not shown here) when the actuator dynamics are introduced in the simulation and hence extra care is needed to address the actuator issue more explicitly.

As expected, the combination of independently rotating wheelset and active control reduces significantly the longitudinal creep forces at the wheel/rail contact point(s) and Table III compares some of the results. On pure curves there is no steady-state creepage for the independently rotating wheelset and the peak creep force on curve transitions is only in the order of tens of Newtons, whereas for the passive vehicle the steady-state creep force on constant curves can be as high as 125 kN. Even for the random track inputs, the creep force of the actively controlled IRW is several times smaller than the passively stabilized solid-axle wheelset.

The control torque required to steer the independently rotating wheelset on pure curved track is very small. Fig. 14 shows the actuator torques on a pure curved track at the vehicle speed of 25 m/s. Even for this tight curve where larger steering action is necessary, the maximum control torque on transition curves is 42 Nm (only about 10 Nm for the high-speed curve of $V_s = 83.3$ m/s) and no steady-state torque is required on the constant curve. However much larger control effort is needed for

TABLE III
VEHICLE PERFORMANCE COMPARISON

		Vehicle Speed (*m/s*)	Passive vehicle with solid-axle wheelsets.	Actively controlled IRW
Longitudinal creep force on random track (rms)		83.3	10.4 kN (front) 8.5 kN (rear)	2.5 kN
Longitudinal creep force on pure curve (steady state)		83.3	13.7 kN 4.1 kN	0 (steady state) 16 N (max.)
Longitudinal creep force on pure curve (steady state)		25	125 kN 89 kN	0 (steady state) 65 N (max.)
Actuator torque on random track		83.3	N/A	1.35 kNm (rms)
Actuator vel. on random track		83.3	N/A	36 m rad/s (rms)
Ride quality, (rms)	Front	83.3	5.30 %g	3.64 %g
	Centre	83.3	4.10 %g	3.12 %g
	Rear	83.3	5.06 %g	3.78 %g
	Overall	83.3	4.86 %g	3.52 %g

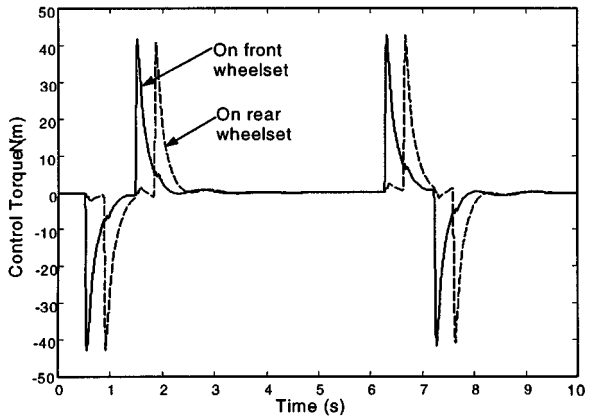

Fig. 14. Control effort on a curved track ($V_s = 25$ m/s).

the wheelsets to respond to the random track input effectively as indicated in Table III. This is particularly true for high-speed applications as the effect of the track roughness becomes worse when the vehicle travels faster. The rms value for each actuator is 1.35 kNm at top vehicle speed, which will decide the actuator size. It should be noted that the overall power requirement of the actuators is fairly low (in the order of tens of Watts per wheelset), because the actuator velocity is only 36mrad/s (rms) at the top speed.

One of the original objectives of the control design is that the active control scheme should also improve the ride quality on the vehicle body (at least it should not deteriorate the passenger comfort). The last four rows of Table III compare the ride quality (body rms accelerations) between the vehicle with actively controlled IRW and the passive vehicle. It is clear from the table that the active control improves the ride quality significantly when compared with the passive vehicle, principally because the kinematic modes of the wheelsets are better controlled and body modes are less affected. The overall ride quality improvement on the vehicle body is 27.5%, with 31% at the front, 24% at the center and 25% at the rear end of the vehicle.

It can be readily shown that it is possible to improve the ride quality further by including the body accelerations as one of the measures in the control design. However the study has shown that a significantly increased control torque will be required which can be disproportionate to the benefit gained on the ride quality.

V. CONCLUSION

This paper has presented the development of an H_∞ control scheme for active steering of independently rotating railway wheelsets. The study has shown that a robust controller with practical sensors can be developed to stabilize the wheelset and to provide necessary guidance control. The control design has been formulated to tackle effectively parameter variations and unmodeled dynamics and the μ-synthesis technique has been used to examine and guarantee the robustness of the closed loop. The robustness achieved has been demonstrated in the computer simulation by using the worst case variations of the wheelset conicity and creep coefficient, as well as full nonlinear models including that for a typical hydraulic actuator and that of the vehicle dynamics with profiled rail and wheels.

It has been demonstrated that with the active control scheme excellent curving and track following of the railway vehicle with independently rotating wheelsets are achieved. The wheel-rail lateral displacements are very small and well within the normal requirement for both curved track and random track inputs, even though these variables are not measured. The longitudinal creepage is significantly reduced due to the combination of the independently rotating wheelset and the effective active control. Simulation results have also indicated that the ride quality on the vehicle body is also improved by 25–30%, compared with the passive vehicle.

In addition the study has shown that the actuator size will be decided by the control requirement for the random track input at the maximum vehicle design speed. Although the torque demand can be as much as 1.35 kNm, the average power requirement will be very low (less than 100 W) because of the low actuator velocity.

REFERENCES

[1] T. X. Mei and R. M. Goodall, "Wheelset Control Strategies for a 2-Axle Railway Vehicle," in *Proc. 16th IAVSD Symp.: Dyn. Vehicles Roads Tracks*, Pretoria, South Africa, 1999.

[2] P. Aknin, J. B. Ayasse, and A. Devallez, "Active steering of railway wheelsets," in *Proc. 12th IAVSD Conf.*, Lyon, France, 1991.

[3] Anon, "A powerful lightweight packed with innovative ideas—single-axle running gear," *BahnTech (research journal of Deutsche Bahn AG)*, vol. 3/97, pp. 4–9, 1997.
[4] A. Powell, R. M. Goodall, C. Walker, D. Nuet, and Y. Noel, "Comparison of the mechanical steering system used on the MF88 trains of the Paris Metro with an active guidance system," in *Proc. Int. Congr. Railtech '98 —Technology for Business Needs*, Birmingham, U.K., Nov. 1998, pp. 85–95.
[5] Anon, "Dosaged torque," *BahnTech (research journal of Deutsche Bahn AG)*, vol. 3/97, pp. 10–11, 1997.
[6] M. Gretzschel and L. Bose, "A Mechatronic approach for active influence on railway vehicle running behavior," in *Proc. 16th IAVSD Symp.—Dyn. Vehicles Roads Tracks*, Pretoria, South Africa, 1999.
[7] A. H. Wickens, "Dynamic stability of articulated and steered railway vehicles guided by lateral displacement feedback," in *Proc. 13th IAVSD Symp.*, Chengdu, China, 1993.
[8] T. X. Mei, R. M. Goodall, and H. Li, "Kalman Filter for the State Estimation of a 2-Axle Railway Vehicle," in *Proc. 5th Europ. Contr. Conf.*, Karlsruhe, Germany, 1999, CA-10-F812.
[9] A. H. Wickens, "The dynamics of railway vehicles—from Stephenson to Carter," *IMechE Proc. (Part F)*, vol. 212, pp. 209–217, 1998.
[10] T. X. Mei, T. H. E. Foo, and R. M. Goodall, "Genetic Algorithms for Optimising Active Controls in Railway Vehicles," in *Proc. Inst. Elect. Eng Colloq. Optimization Contr.: Methods Applicat.*, London, U.K., 1998, (98/521).
[11] S. Skogestad and Postlethwaite, *Multivariable Feedback Control*. London, U.K.: Wiley, 1996.
[12] V. K. Garg and R. V. Dukkipati, *Dynamics of Railway Vehicle Systems*. New York: Academic, 1984, pp. 103–134.

T. X. Mei received the B.Sc. and M.Sc. degrees from Shanghai Institute of Railway Technology in 1982 and 1985, respectively, the M.Sc. degree from Manchester University, U.K., in 1991, and the Ph.D. degree from Loughborough University, U.K., in 1994.

He held an academic position in the department of Electrical Engineering at Shanghai Institute of Railway Technology between 1985 and 1989. From 1993 to 1998, he worked in industry in the United Kingdom, responsible for the success of many industrial R&D projects. From 1998 to 2000, he was a Senior Research Engineer at Loughborough University. He currently holds an academic position in the School of Electronic and Electrical Engineering at the University of Leeds. His research is concerned with a variety of practical applications of advanced control, including motor drives, traction control, vehicle dynamics, contact mechanics, excitation control, fault-tolerant systems, system integration, and real-time implementations.

Dr. Mei is a member of the Institute of Electrical Engineers and a Chartered Engineer.

Roger M. Goodall received the M.A. degree from Cambridge University (Peterhouse), Cambridge, U.K., in 1968.

After working for two years for one of the GEC companies he joined British Rail's R&D Division, where he was involved in a variety of control-related projects connected with the railway industry. In 1982, he took up an academic position in the Department of Electronic and Electrical Engineering at Loughborough University, and is currently Professor of Control Systems Engineering. His research is concerned with a variety of practical applications of advanced control, usually for high-performance electro-mechanical systems. He holds a number of research grants from EPSRC, the EC and industry concerned with active railway vehicle suspensions, advanced data fusion architectures for aerospace applications, and targetted processor architectures for implementation of high-performance controllers.

Dr. Goodall is a Fellow of both the Institute of Electrical Engineers and IMechE, and has received a number of awards from both these institutions for his published work.